

Supplementary Information

The Contrasting Catalytic Efficiency and Cancer Cell Antiproliferative Activity of Stereoselective Organoruthenium Transfer Hydrogenation Catalysts

Ying Fu, Carlos Sanchez-Cano, Rina Soni, Isolda Romero-Canelón, Jessica M. Hearn, Zhe Liu, Martin Wills, and Peter J. Sadler

Tables S1 – S5

Figures S1 – S9

Table S2COMPARE results using NCI/DTP synthetic agents database for the GI₅₀ endpoint

8			8a		
Correlated agent	PCC	Mechanism	Correlated agent	PCC	Mechanism
MW03	0.868	-	MW02	0.868	-
Pleurotin	0.661	Inhibit flavoprotein thior edoxin reductase Inhibits hypoxia induced increase of HIF-1a	Eupacunoxin	0.673	
Mercaptoacetate	0.654	Potential DNA cleavage	Bipinnatin H	0.664	
Zinolide	0.652	No data on MoA	Mercaptoacetate	0.664	Potential DNA cleavage
Xestoquinone	0.649	Topo II mediated DNA cleavage	Urdamycin A, pentaacetate	0.659	
Cryptosporiopsin	0.649	Inhibit RNA synthesis by altering nucleotides. Also disrupts production of ATP.	Arnebin 1	0.658	
Methyl-CCNU	0.642	Alkylating agent	Mikanolide	0.656	
Eupacurvin	0.636	No data on MoA	Multistatin	0.652	
Urdamycin A, pentaacetate	0.614		Gold, chloro(triethyl phosphine)	0.65	
Homopterocarpin	0.605		Straital B	0.65	
			Acnistin F	0.648	
			Cryptosporiosin	0.647	Inhibit RNA synthesis by altering nucleotides. Also disrupts production of ATP.
			Heliangolide	0.645	
			Eupacurvin	0.645	
			Withaferin A	0.643	

NCI/DTP database. Only those agents returned within the first 100 correlations, with (PCC) > 0.6 are shown. Agents with compound names, and not registered names, are omitted.

Table S3

COMPARE results using NCI/DTP synthetic agents database for the TGI endpoint

8			8a		
Correlated agent	PCC	Mechanism	Correlated agent	PCC	Mechanism
MW03	0.945	-	MW02	0.874	-
Mercaptoacetate	0.656	Potential DNA cleavage	Mercaptoacetate	0.695	Potential DNA cleavage
			Gold, chloro(triethyl phosphine)	0.638	
			Arnebin 1	0.614	
			Straital B	0.610	
			Santolinapolyacetaylene 18	0.602	

NCI/DTP database. Only those agents returned within the first 100 correlations, with PCC > 0.6 are shown. Agents with only their compound structure name, and not registered names, are omitted.

Table S4

COMPARE results using the NCI/DTP synthetic agents database for the LC₅₀ endpoint

8			8a		
Correlated agent	PCC	Mechanism	Correlated agent	PCC	Mechanism
MW03	0.942	-	MW02	0.942	-
Withaferin A	0.847				
Mercaptoacetate	0.809	Potential DNA cleavage	Withaferin A	0.73	
Urdamycin A, pentacetate	0.793		Longikaurin B	0.727	
Kalafungin(USAN)	0.785		Eupachlorin acetate	0.727	
T 1(VAN)	0.773		Cumertilin	0.723	
Longikaurin B	0.765		Celastrol	0.684	
Stannane, dibutylidithiocyanato	0.761		Acetyl rolandrolide	0.682	
Cumertilin	0.739		Iso-withanolide E 14,15-epoxy-6 alpha	0.662	
Helenine	0.736		Alpha-bromochalcone	0.653	
ChelerythrineHCl	0.73		Cleandrin	0.653	
Secalone B	0.726		Arylpurine derivatives	0.65	
Farinosin, dehydro	0.72				
Plumbaein	0.715				
Celastrol	0.712				
Sanguinarine Nitrate	0.71				

NCI/DTP database. Only those agents returned within the first 100 correlations, with PCC > 0.6 are shown. Agents with compound names, and not registered names, are omitted.

Table S5

Values for the cell cycle analysis using flow cytometry experiments in A2780 ovarian cancer cells. All values are compared to the untreated controls for statistical significance calculations.

Sample	Cell cycle	Averages	Stdev	P-value against -ve
Controls	Sub-G1	0.000	0.000	
	G1	62.700	0.854	
	S	23.167	0.751	
	G2/M	10.703	0.362	
Colchicine (100 nM)	Sub-G1	12.400	0.436	0.000411643
	G1	7.553	0.832	1.46989E-07
	S	13.433	0.551	0.000100684
	G2/M	55.933	2.325	0.000683922
Taxol (100 nM)	Sub-G1	22.933	1.701	0.001828733
	G1	17.300	1.153	1.66939E-06
	S	11.433	0.907	8.43193E-05
	G2/M	45.600	1.473	0.000306016
7 (2 μ M)	Sub-G1	3.305	0.601	0.081418053
	G1	57.950	0.636	0.007032042
	S	29.000	0.849	0.014886727
	G2/M	15.050	0.778	0.051306728
7a (2 μ M)	Sub-G1	4.360	0.740	0.00946604
	G1	46.533	3.647	0.012960242
	S	30.300	1.114	0.001410555
	G2/M	20.033	2.470	0.020725302
8 (2 μ M)	Sub-G1	13.750	0.354	0.01157363
	G1	54.500	0.283	0.001328262
	S	17.950	0.778	0.013337581
	G2/M	17.300	0.566	0.011716941
8a (2 μ M)	Sub-G1	2.683	0.163	0.001221477
	G1	56.600	0.624	0.000870273
	S	22.667	1.026	0.536401588
	G2/M	16.700	1.253	0.009689256

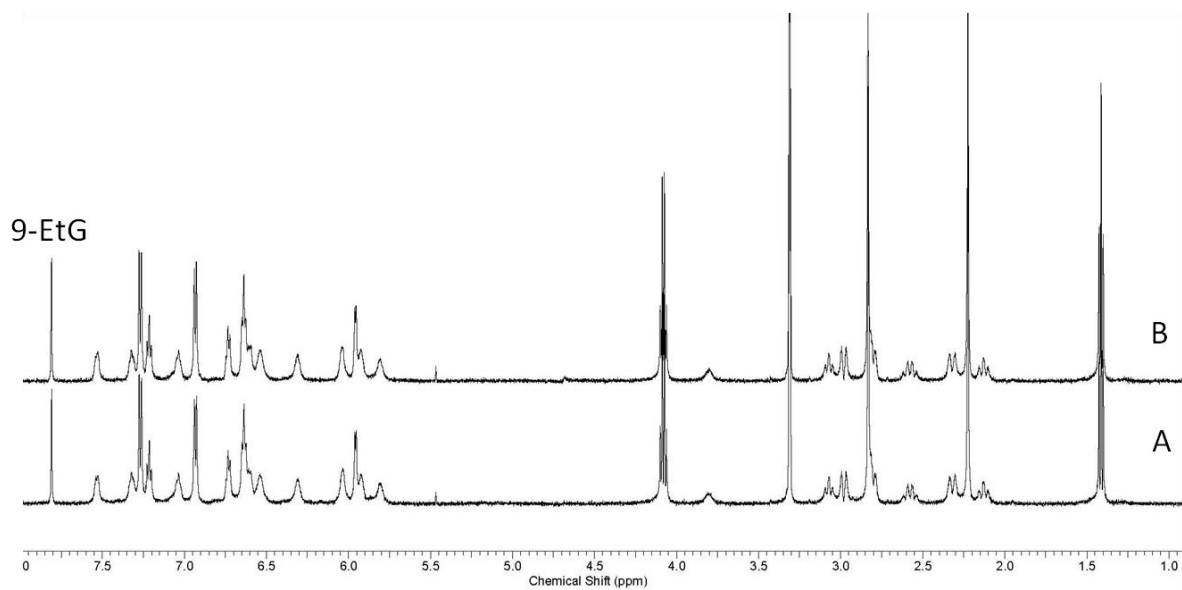


Figure S1. ¹H NMR spectra of **8a** (1.5 mM) and 9-EtG (1.5 mM) in 25% MeOD-*d*₄/75% D₂O (v/v) at 310 K after (A) 10 min and (B) 24 h.

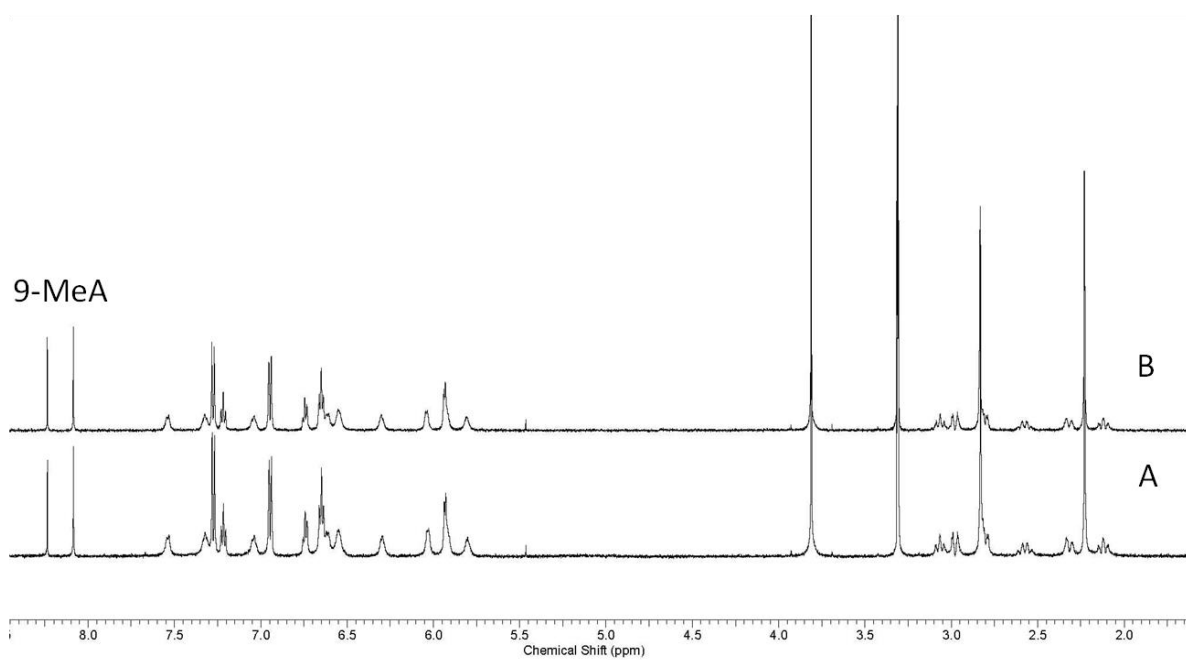


Figure S2. ¹H NMR spectra of **8a** (1.5 mM) and 9-MeA (1.5 mM) in 25% MeOD-*d*₄/75% D₂O (v/v) at 310 K after (A) 10 min and (B) 24 h.

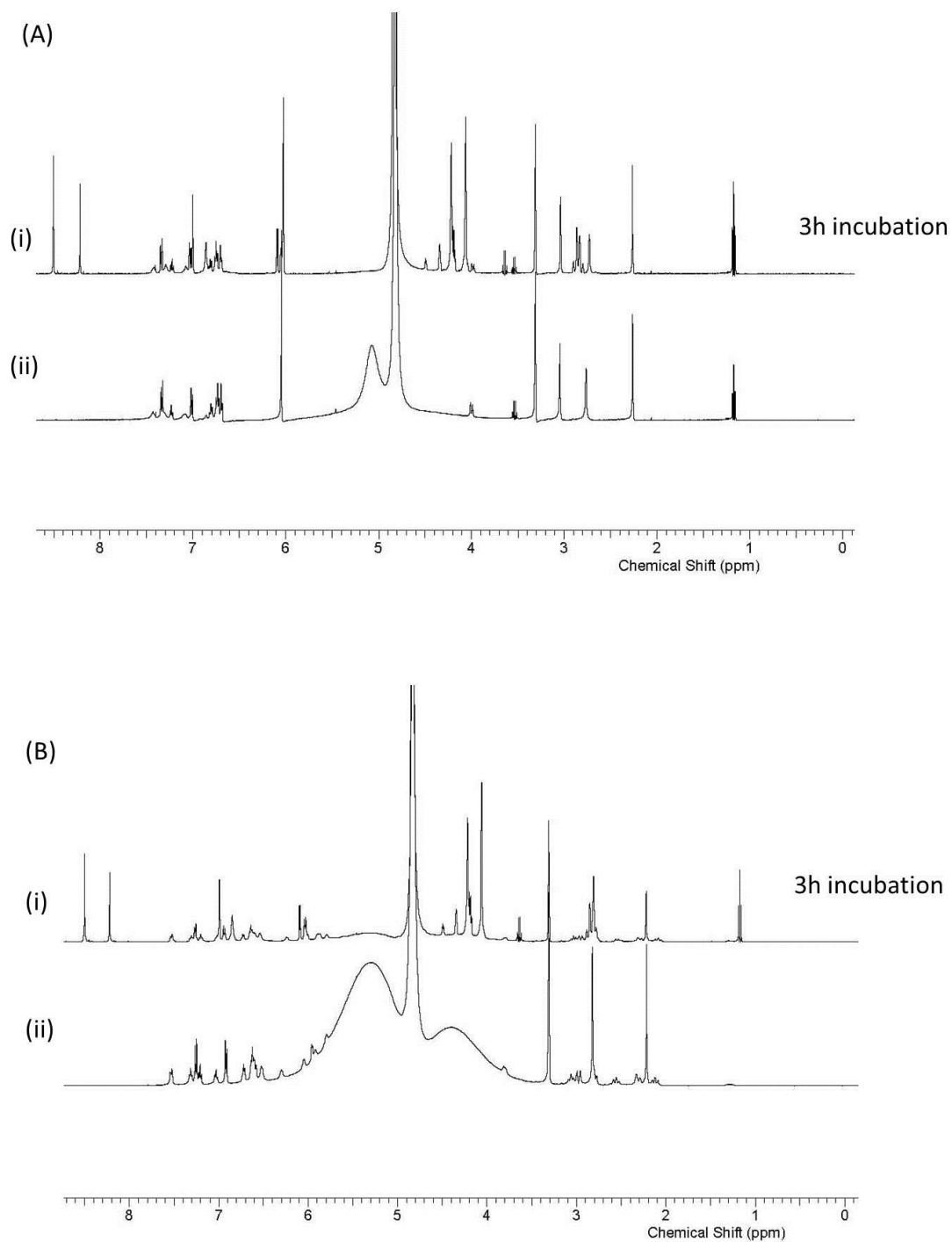


Figure S3. ^1H NMR spectra of **7** (A) and **8a** (B) with NADH in 25% $\text{MeOD-}d_4/75\%$ D_2O (v/v) at 298 K: (i) equilibrium solution of the complexes (1.5 mM); (ii) 3 h after addition of 3 mol equiv of NADH to the above solution. No reaction between the complexes and NADH was observed after 3 h incubation. The broad humps in (ii) arise from incomplete H_2O peak suppression.

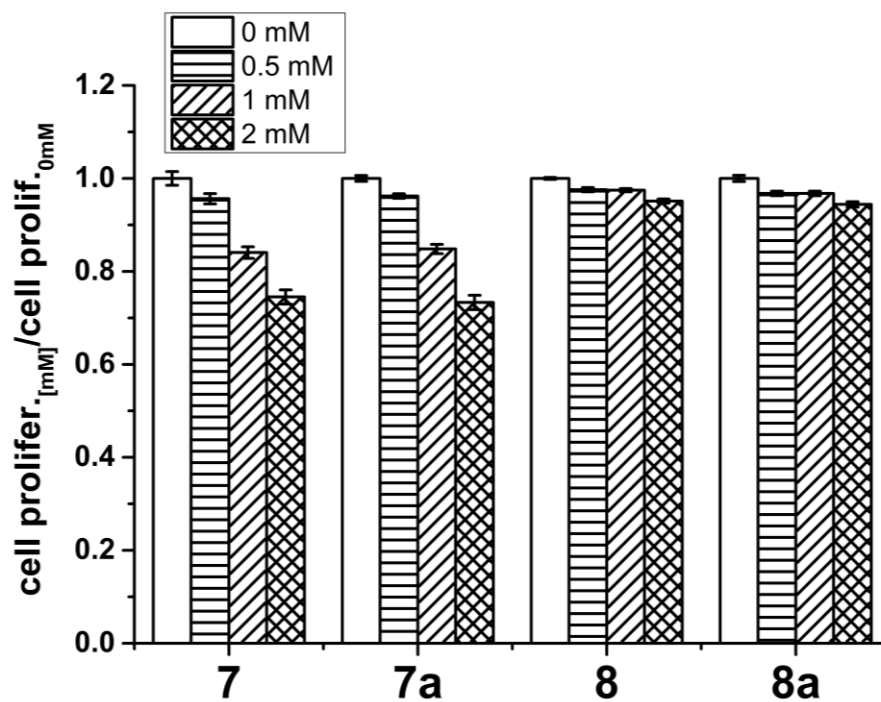


Figure S4. Effect of co-administration of sodium formate (0, 0.5, 1 or 2 mM) and complexes **7/8** ($1/5$ IC_{50}) on cell survival.

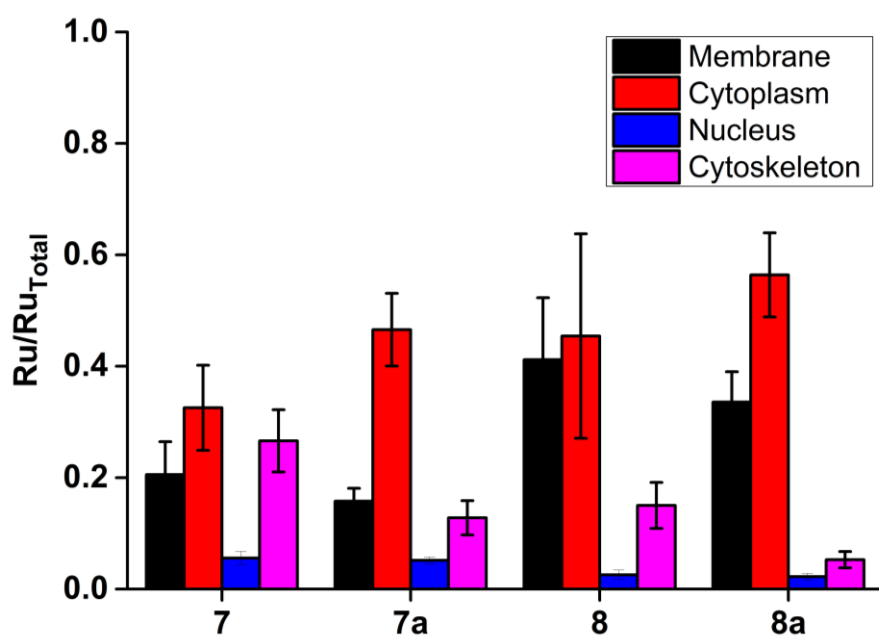


Figure S5. Relative distribution of ruthenium in the different cellular fractions of A2780 ovarian carcinoma cells (expressed in ng Ru/million cells) after 24 h treatment with 2 μ M of **7/8**.

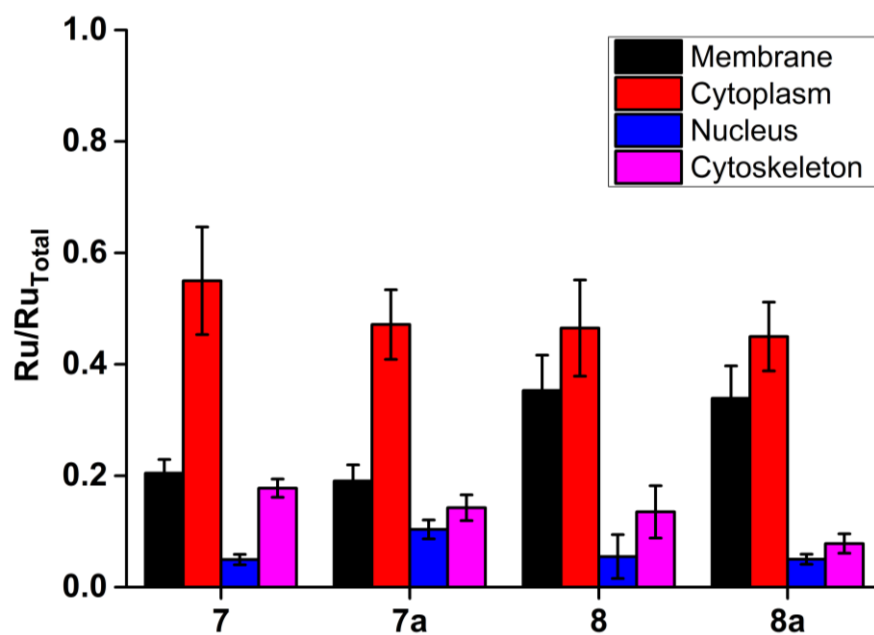


Figure S6. Relative distribution of ruthenium in the different cellular fractions of A2780 ovarian carcinoma cells (expressed in ng Ru/million cells) after 24 h treatment with IC₅₀ concentration of **7/8**.

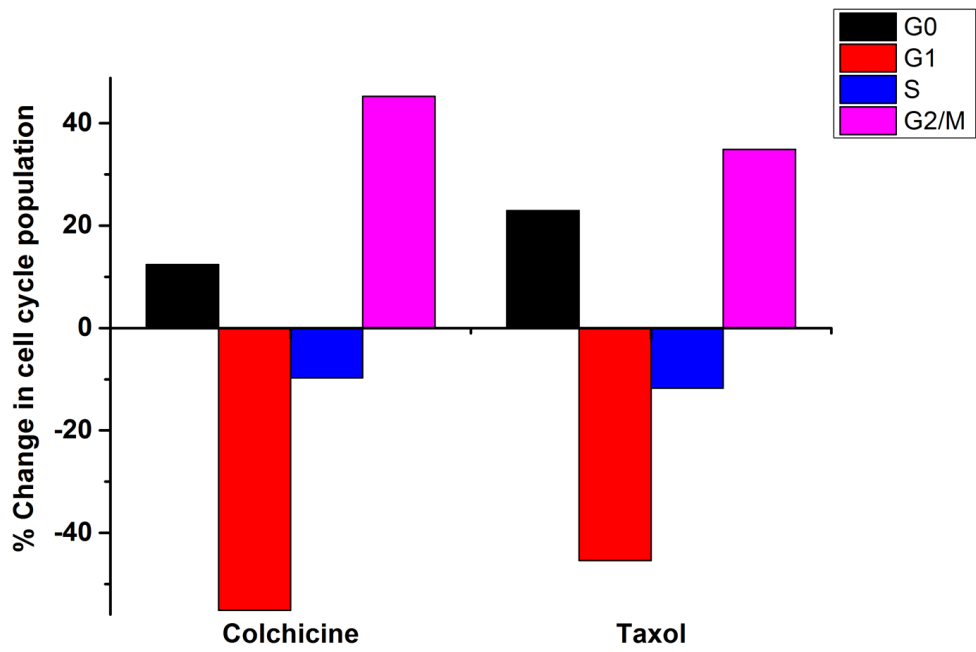


Figure S7. Changes in the cell cycle of A2780 ovarian carcinoma cells after 24 h treatment with 100 nM of Colchicine or Taxol.

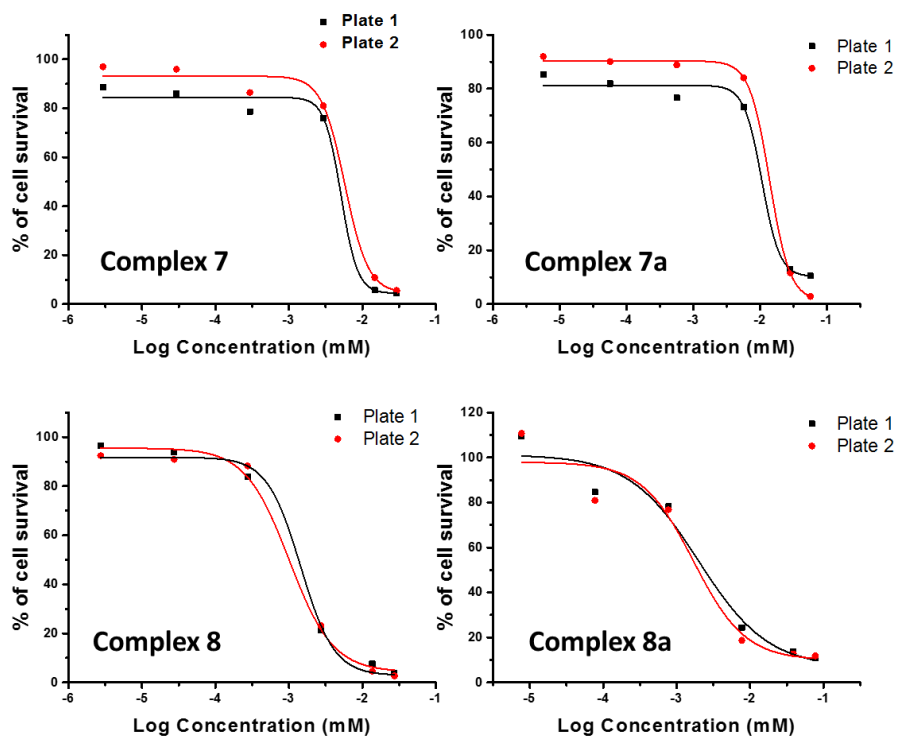


Figure S8. Cell viability test of A2780 ovarian carcinoma cells treated with ruthenium complexes (7, 7a, 8, 8a).

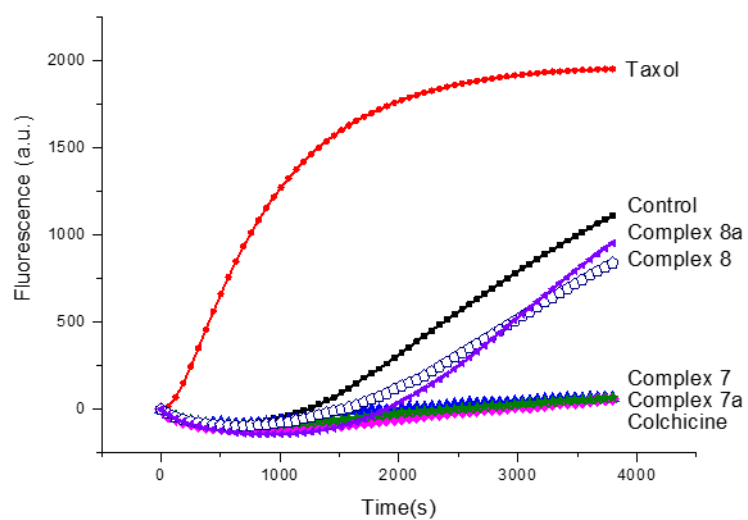


Figure S9. Kinetics of tubulin polymerisation at 310 K : untreated (■), complex 7 (◆, 10 μM), complex 7a (★, 10 μM), complex 8 (◊, 10 μM), complex 8a (▲, 10 μM), Taxol (●, 3 μM, stabilises microtubules) and Colchicine (▲, 3 μM, inhibits microtubule formation). Microtubule formation was monitored by the increase in fluorescence (arbitrary units) of a reporter incorporated into microtubules as polymerisation proceeds.